

Time Domain and Frequency Domain Analysis for Truss Spar Platform

O.A.A. Montasir¹, V.J. Kurian²

Universiti Teknologi PETRONAS, MALAYSIA

ABSTRACT

The spar platforms for offshore oil exploration and production in deep and ultra deep waters are increasingly becoming popular. A number of concepts have evolved, among them the ‘classic’ spar and “truss” spar being the most prevalent. Time domain and frequency domain analysis were used to determine the dynamic responses for a typical truss spar platform. The hyperbolic extrapolation wave theory and modified Morison Equation were used for simulating the sea state and for determining the dynamic force vector. The platform was modeled as a rigid body with three degrees of freedom, surge, heave, and pitch restrained by mooring lines. In time domain, Newmark Beta method was used to solve the equation of motion. Static offset tests were numerically conducted to obtain the mooring line stiffness curves. In frequency domain analysis, the steady state responses were obtained. Time domain results were compared to frequency domain results in terms of response amplitude operator. These results were discussed and compared with numerical and experimental results in the available literature.

Keywords: spar; dynamic analysis; time domain; frequency domain; hydrodynamic responses; rigid body; mooring lines

1. *PhD. Student, Civil Engineering Department, Universiti Teknologi PETRONAS, 31750 Tronoh, Perak, Darul Ridzuan Malaysia. Tel: +6017-5701471, E-mail: montaserageeb@yahoo.com*

2. *Professor, Civil Engineering Department, Universiti Teknologi PETRONAS, 31750 Tronoh, Perak Darul Ridzuan Malaysia. Tel: +605-3687345, E-mail: jokurian26@yahoo.com*

1. INTRODUCTION

The spar platforms for offshore oil exploration and production in deep and ultra deep waters are increasingly becoming popular. A number of concepts have evolved, among them the ‘classic’ spar and ‘truss’ spar being the most prevalent. The classic spar has an upper buoyant cylindrical hard tank, a keel ballast tank (soft tank) and a flooded cylindrical midsection. The long midsection has large diameter and its design is mostly governed by construction loads. The spar platform is very cost-ineffective. In the late 1990s, development of truss spar concept advanced much with a large amount of research effort in model test [1,2], and theoretical study [3,4,5]. Since then, ten truss spars have been designed, constructed and/or installed.

The truss spar consists of a top hard tank and a bottom soft tank separated by a truss midsection. The soft tank mainly contains solid ballast to provide stability, whereas the hard tank provides buoyancy and contains trim ballast. The truss section contains a number of horizontal heave plates designed to reduce heave motion by increasing both added mass and hydrodynamic damping.

Several analytical or numerical approaches can be used to calculate the dynamic response of spars. The most direct approach is the analysis in the time domain, where a wave elevation time series is used as input and the resulting structural responses are calculated numerically. This allows direct comparison with experimental time series response. However, this is usually quite expensive, and tells little about the nature of the vibration. An approximate but less expensive approach is to conduct the analysis in frequency domain, which gives only the steady state responses that can be converted back to time domain.

In the structural analysis in time domain, it is common practice to treat the mooring lines and risers as springs. This neglects the inertia of the mooring system, as well as the additional drag forces that may increase the damping of the total structure. The static offset tests were conducted numerically by applying variable static forces and from these tests, mooring stiffness curves were obtained.

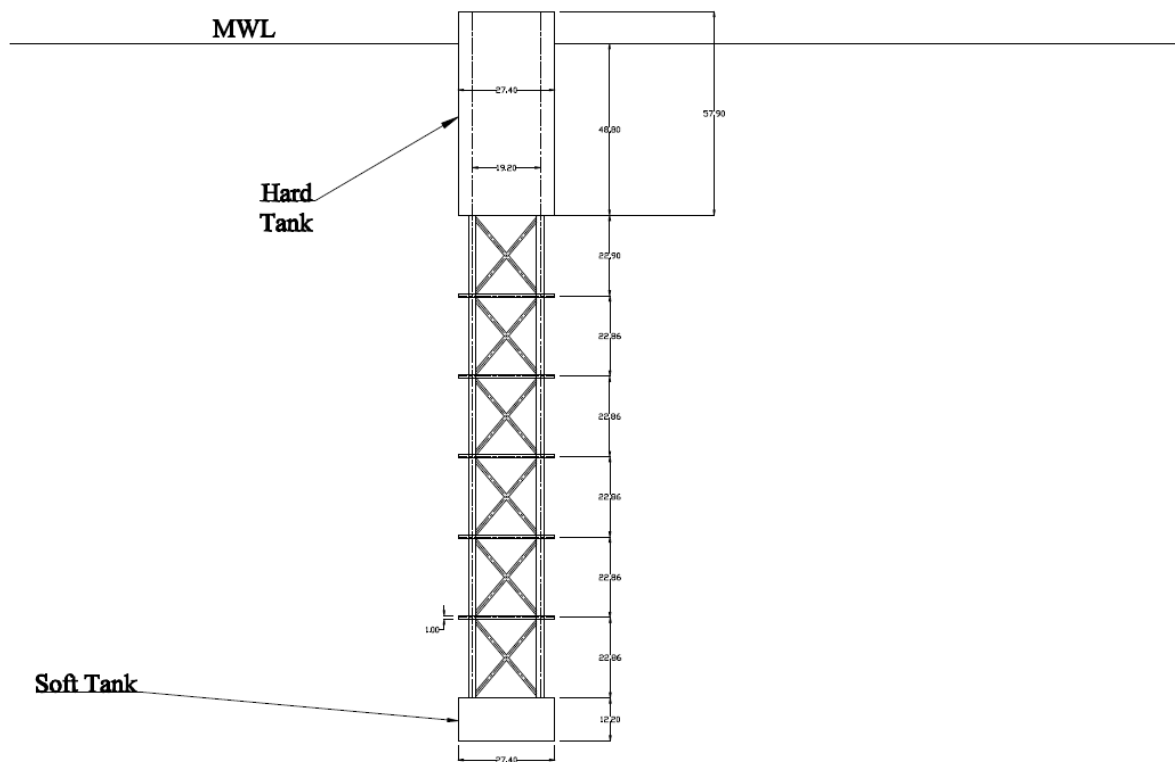
A MATLAB program named ‘TRSPAR’ was developed to determine the responses in time domain. Numerical integration using Newmark Beta method was employed and the platform was modeled as a rigid body with three degrees of freedom restrained by mooring lines affecting

the stiffness values. Hyperbolic extrapolation formula and modified Morison equation were used for simulating the sea state and for determining the dynamic force vector. Added mass and damping were derived from hydrodynamic considerations.

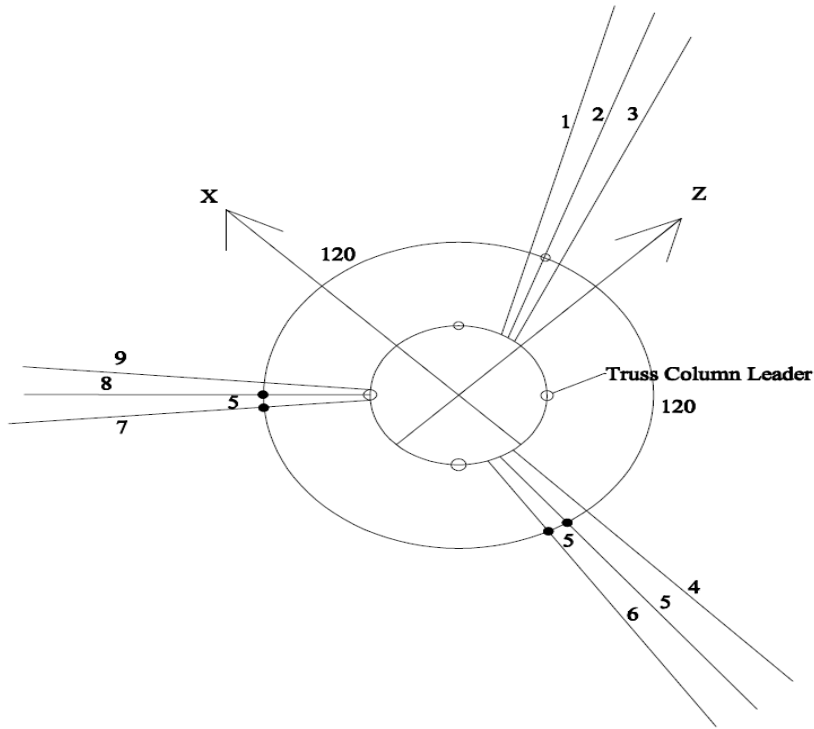
Time domain results were compared with frequency domain results in terms of response amplitude operator. These results were compared with both a set of laboratory model test results and a set of numerical analysis results reported in the literature.

2. NUMERICAL METHOD

Numerical simulation was conducted for Amoco Marlin truss spar which was positioned by nine taut mooring lines [Fig. 1] in 988 m water depth.



Overall Spar Configuration



Amoco Marlin Truss Spar Mooring Arrangement

Fig. 1: Amoco Marlin truss spar

2.1 Analysis of Mooring Line

The force–excursion relationship is nonlinear and requires an iterative solution. Equation of a catenary was used for evaluation of force-excursion relationship of a taut mooring line [9]. The horizontal projection and vertical projection of any segment hanging freely under its own weight w per unit length as shown in Fig. 2 can be expressed (considering horizontal force (H_t), top slope (θ_t), length (S) and weight (W)) as:

$$Y = (H_t / W)[\cosh\{\sinh^{-1}(\tan(\theta_t))\} - \cosh\{\sinh^{-1}(\tan(\theta_b))\}] \quad (1)$$

$$X = (H_t / W)[\sinh^{-1}(\tan(\theta_t)) - \sinh^{-1}(\tan(\theta_b))] \quad (2)$$

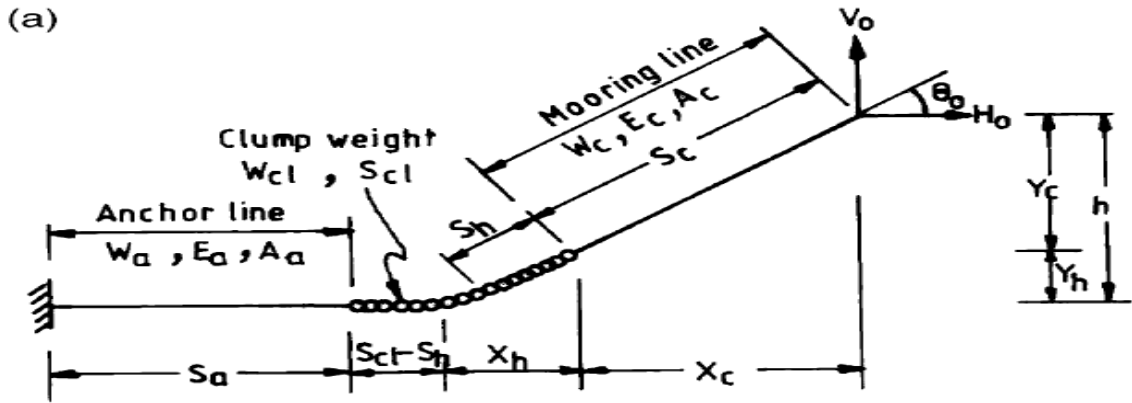
$$\tan(\theta_b) = (V_t - WS) / H_t \quad (3)$$

$$V_t = H_t \tan(\theta_b)$$

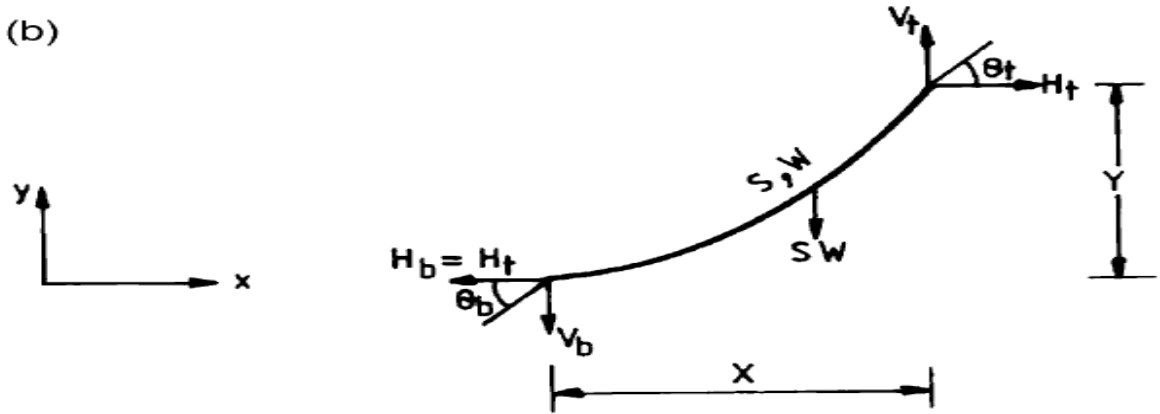
When for any segment the bottom slope (θ_b) is zero, the above equation reduces to:

$$Y = (H_t / W)[\cosh\{\sinh^{-1}(\tan(\theta_t))\} - 1] \quad (4)$$

$$X = (H_t / W)[\sinh^{-1}(\tan(\theta_t))] \quad (5)$$



(a) Initial configuration with different sectional



(b) Free body diagram of uniform mooring line suspended freely between two points not in the same elevation.

Fig. 2. Multi component mooring line

If H_t, Y, W, θ_t are known then,

$$\tan(\theta_b) = \sinh[\cosh^{-1}[\cosh\{\sinh^{-1}(\tan(\theta_t))\} - (YW/H_t)]] \quad (6)$$

$$S = H_t(\tan(\theta_t) - \tan(\theta_b)) / W \quad (7)$$

and X can be evaluated by Eq.(2).

The extension of any segment under increased line tension can be approximately evaluated as follows. Let the initial average line tension be T_0 when the segment length is S_0 . For increased average line tension T , the stretched length becomes:

$$S = S_0[1 + (T - T_0) / EA] \quad (8)$$

where, E and A are the Young's modulus and effective area of the segment respectively.

T and T_0 is the arithmetic means of the line tensions at two ends. The total weight of any segment (W) remains same,

$$W = (S_0 W_0) / S \quad (9)$$

where W is the modified unit weight due to stretching and W_0 is the unit weight of the unstretched segment.

If H_0 , θ_0 , h , zero bottom slope and the elastic and physical properties of the segments, as shown in Fig. 3(a), are chosen as the known parameters. The unknowns which are to be evaluated are S_c , S_h and then Y_c , Y_h , X_c and X_h .

The following steps are used to find the unknowns given above.

Step 1 Calculate V_0 from the known values of H_0 and θ_0 .

Step 2 Find the slope at the junction of the clump weight and mooring line, then find vertical force at the junction V_j (which will be equal to $S_h W_c l$ as the bottom slope is equal to zero).

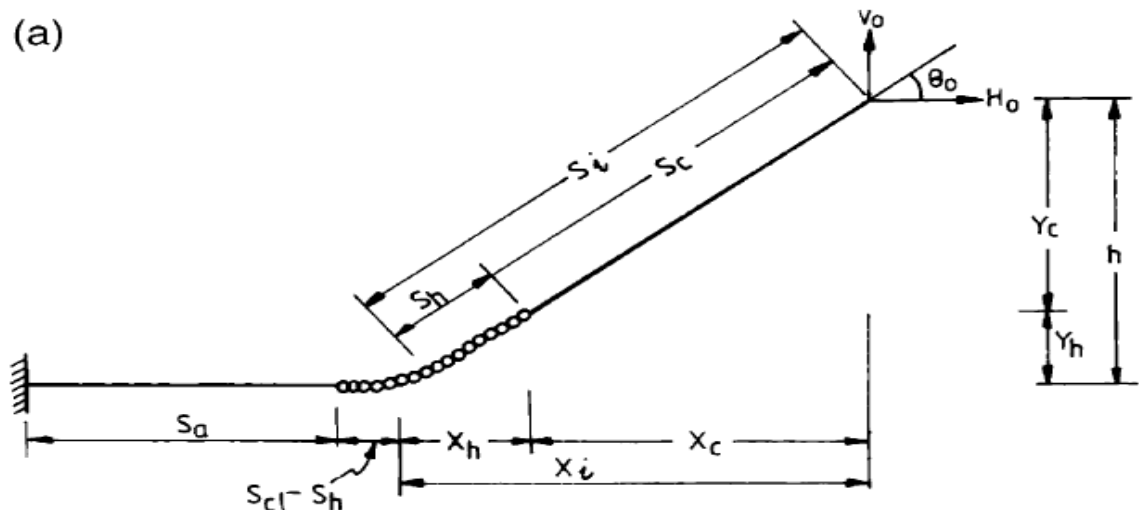
Using the known values of the horizontal force, use Eq. (4) to find Y_h .

Step 3 Find $S_c = (V_0 - S_h W_c l) / W_c$ and then find Y_c using Eq. (1).

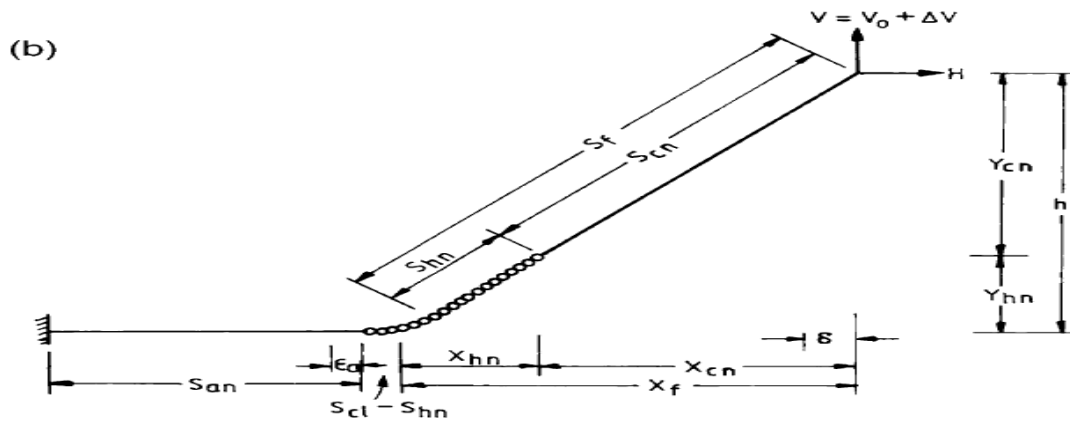
Step 4 Add up Y_c and Y_h and compare with h . If the difference is less than a specified limit, go to the next step, otherwise change V_j appropriately and repeat the procedure from step 2.

For the first iteration the change of V_j can be taken as $\pm 1\%$ depending upon the sign of error. For the subsequent iterations the following equation is to be used to get a new value of V_j .

$$(V_j)_{k+1} = (V_j)_k - [e_k((V_j)_{k-1} - (V_j)_k) / (e_{k-1} - e_k)]$$



(a) Initial configuration.



(b) Final configuration.

Fig. 3. Configuration of mooring line for increased horizontal force, H .

where, k is the number of the last iteration, $(V_j)_k$ is the vertical force at the junction of the mooring line and clump weight and e_k is the difference between the vertical projection of the hanging length of the mooring line calculated in the k^{th} iteration and the mooring level (h).

Step 5 Find X_c and X_h from Eqs. (2) and (5), respectively.

Step 6 Find initial total hanging length $S_i = S_c + S_h$ and its horizontal projection $X_i = X_c + X_h$.

For an excursion of δ at the attachment point the resultant horizontal force is given by:

$$H(\delta) = \sum_{j=1, p} H_j(\delta_j) \cos(\pi - \theta_j) \quad (10)$$

where p is the total number of mooring lines, θ_j the angle between the j th mooring line and the direction of excursion. δ_j is the excursion for the j th mooring line and $H_j(\delta_j)$ is the associated horizontal force, with $\delta_j = \delta \cos(\pi - \theta_j)$.

The particulars for the multi component taut mooring line are given in Table 1.

Table 1. Characteristics of prototype mooring

	Upper section	Middle section	Lower section
type	K4 Chain	Spiral strand	K4 Chain
Size (cm)	12.4	12.4	12.4
Length outboard (m)	76	1829	46
Wet weight (Kg/m)	278	65	278
Eff. Modulus EA (Kn)	666×10^3	1.34×10^6	859×10^3
Breaking strength (Kn)	13.2×10^3	12.5×10^3	13.2×10^3

2.2 Time Domain Analysis

The nonlinear time domain numerical model performed step-by-step numerical integration of the exact large amplitude equation of motion, producing time histories of motions. The fluid forces on individual members were computed by the modified Morison equation in which the integration of the forces was performed over the instantaneous wetted length. The total force at each time step was obtained by summing the forces on the individual members. Incident wave kinematics was calculated by using hyperbolic extrapolation formula. A numerical model for a truss spar was developed that was able to predict the dynamic responses at any instant.

Considering that the incident waves were long crested and were advancing in the x-direction, the truss spar was approximated by a rigid body of three degrees of freedom (surge, heave and pitch), deriving static resistance from support systems (mooring lines) and hydrostatic stiffness.

As shown in Fig. 4, two coordinate systems were employed in the analysis [6], the space fixed coordinate system oxz and two dimensional local coordinate $G\zeta\eta$ which was fixed on the body with the origin at its center of gravity (CG). The point B denoted the center of buoyancy and point F denoted fairlead.

The space-fixed coordinates were related to the body-fixed coordinates by:

$$\begin{Bmatrix} x \\ z \end{Bmatrix} = \begin{Bmatrix} 0 \\ -d \end{Bmatrix} + \begin{Bmatrix} X_g \\ Z_g \end{Bmatrix} + \begin{Bmatrix} \cos \theta & \sin \theta \\ -\sin \theta & \cos \theta \end{Bmatrix} \begin{Bmatrix} \zeta \\ \eta \end{Bmatrix} \quad (11)$$

Where X_g , Z_g denoted surge and heave motions at G and θ denoted the pitch angle about the y-axis considered positive clockwise. The coordinates of G at its mean position in calm water were given by (0,-d).

The wave forces on the hard tank were decomposed into the normal force F_{EXn} (normal to the centerline) and tangential force F_{EXt} (along the centerline). The normal wave force was determined using Morison equation at the instantaneous position of the structure and integrating along its centerline from the bottom of the hard tank (0,-d₁) to the free surface $\zeta(t)$ in body-fixed coordinate system $\xi G \eta$.

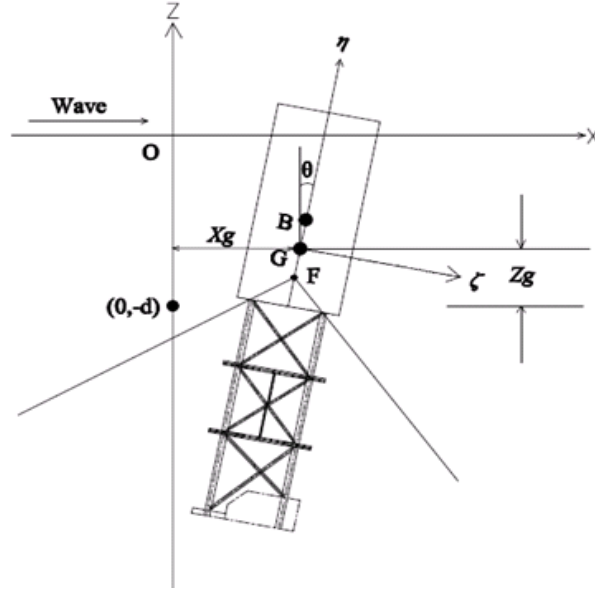


Fig. 4: Three-DOF model of the spar

$$\begin{Bmatrix} F_{EXn} \\ M_{EX} \end{Bmatrix} = \int_{-d_1}^{\zeta(t)} \rho(1 + C_m)A(n)a_n \begin{Bmatrix} 1 \\ n \end{Bmatrix} dn + \int_{-d_1}^{\zeta(t)} \frac{1}{2} \rho C_D D |V_n| V_n \begin{Bmatrix} 1 \\ n \end{Bmatrix} dn + \int_{-d_1}^{\zeta(t)} \rho C_m A(n) V_n \tau^T v \tau \begin{Bmatrix} 1 \\ n \end{Bmatrix} dn \quad (12)$$

Where

$$a_n = |a - (a \cdot \vec{\tau}) \vec{\tau}|$$

$$V_n = |V - r_s - ((V - r_s) \cdot \vec{\tau}) \vec{\tau}|$$

$$\tau = \begin{bmatrix} \sin \theta \\ \cos \theta \end{bmatrix}$$

C_m was the added mass coefficient, C_D the drag coefficient, V_n the relative normal velocity, and $\vec{\tau}$ the unit vector along the η axis. a and V were the wave particle acceleration and velocity respectively, and r_s was structure velocity. The last term in Eq. 12, described Rainey's normal axial divergence correction in which the velocity gradient matrix was given by:

$$v = \frac{\partial(u, w)}{\partial(x, z)} \quad (13)$$

The tangential force could be determined by integrating the hydrodynamic pressure on the bottom surface S_B

$$F_{EXt} = \iint_{S_b} \rho \frac{\partial \phi^{(1)}}{\partial t} + \frac{1}{2} \rho |\nabla \phi^{(1)}|^2 n_t \partial S \quad (14)$$

Where $\phi^{(1)}$ was the first potential of incident waves which could be computed using linear Airy theory.

Forces FEXn and FExt were transferred into spaced-fixed coordinate system oxz as:

$$\begin{Bmatrix} F_{EXx} \\ F_{EXz} \end{Bmatrix} = \begin{Bmatrix} \cos \theta & \sin \theta \\ -\sin \theta & \cos \theta \end{Bmatrix} \begin{Bmatrix} F_{EXn} \\ F_{EXt} \end{Bmatrix} \quad (15)$$

The equation of motion was solved by an iterative procedure using unconditionally stable Newmark's Beta method. The program 'TRSPAR' included a provision for calculating the values of drag and inertia hydrodynamic coefficients at any point of the structure and at any instant, based on the KC (Keulegan-Carpenter) parameter. The charts provided by Chakrabarti [7] based on wave tank tests done on a cylinder, were made use of.

The response amplitude operator (RAO) was written as

$$\text{RAO} = \text{Response}(t) / \eta(t) \quad (16)$$

Where $\eta(t)$ was the wave profile as a function of time t.

2.3 Frequency Domain Analysis

Because the contribution of the drag force was very small compared to the inertia force; the drag term was neglected in the frequency domain analysis.

The steady state response vector $x(t)$ was given by

$$x(t) = \left[\frac{F_I / (H/2)}{[(K - Mw^2)^2 + (Cw)^2]^{1/2}} \right] \eta(t) \quad (17)$$

Where

F_I , H , K , M , w , and C were the inertia force, wave height, stiffness matrix, mass matrix, wave frequency, and damping matrix respectively.

3. RESULTS AND DISCUSSION

Based on the mooring lines analysis method, mooring stiffness curves were obtained, as shown in Fig. 5. The calculated mooring stiffness shows nonlinear “hardening” behavior.

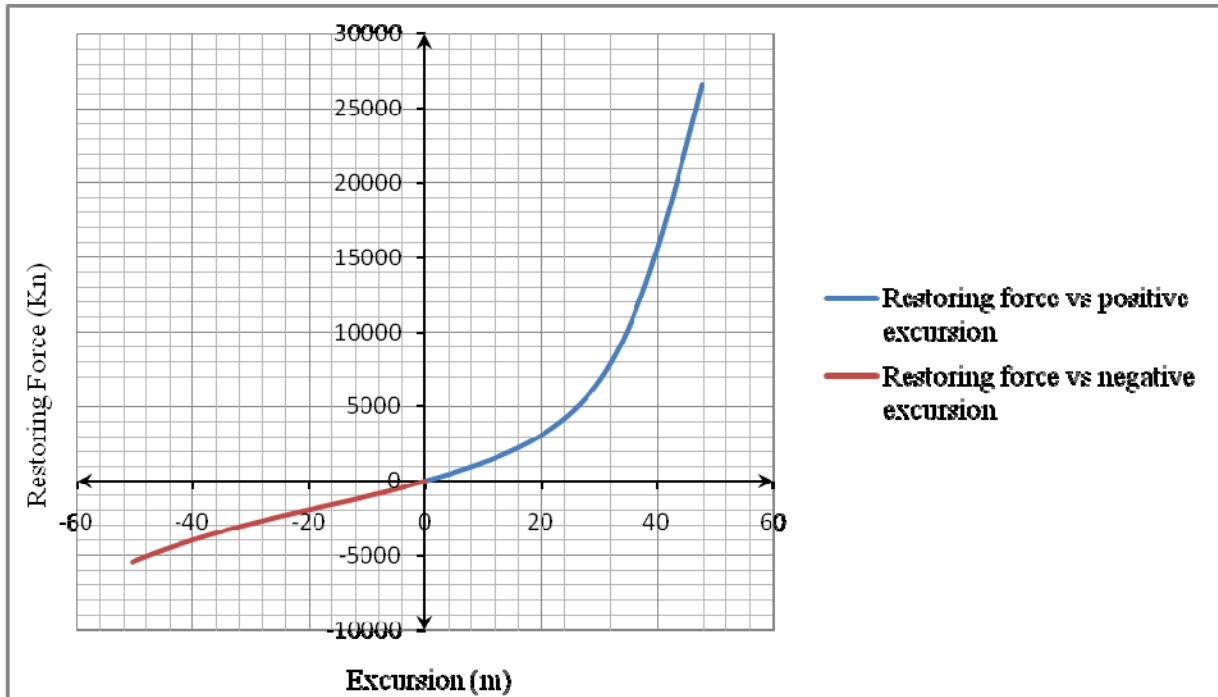


Fig. 5: Surge static offset simulation

The responses of truss spar were determined numerically using two different approaches, which were time and frequency domain analysis, and the results were compared with the corresponding results computed using a Time Domain numerical simulation code called TDSIM [8] and model test measurements.

The surge RAOs for time and frequency domain agreed well as shown in Fig 6. For higher wave periods, frequency domain gave lower surge values compared to time domain analysis. ‘TRSPAR’ surge results agreed very well with the corresponding ‘TDSIM’ results and the model test measurements.

The heave RAO for ‘TRSPAR’ compared well with the corresponding results of ‘TDSIM’ and the model test measurements as shown in Fig. 7. The heave RAO for the frequency domain analysis compared well with the corresponding results of ‘TRSPAR’, ‘TDSIM’ and the model

test measurements for low wave periods but it gave different trend for higher wave periods.

The pitch RAO for 'TRSPAR', frequency domain, 'TDSIM', and model test measurements agreed well as shown in Fig. 8.

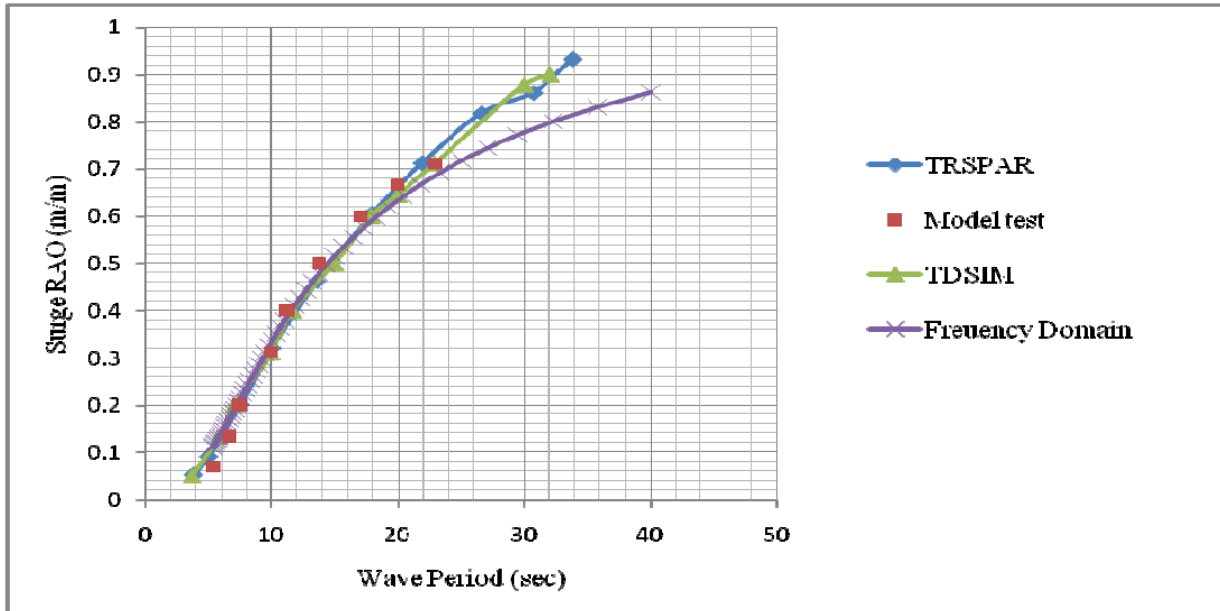


Fig. 6: Comparison of surge RAO at zero degree heading

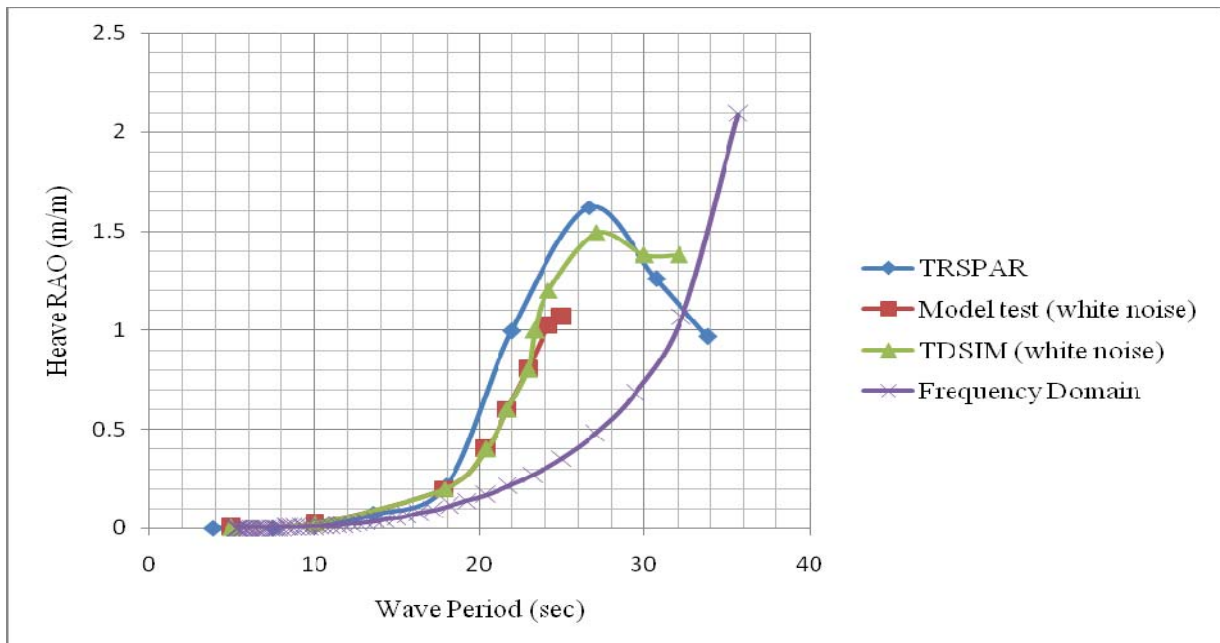


Fig. 7: Comparison of heave RAO at zero degree heading

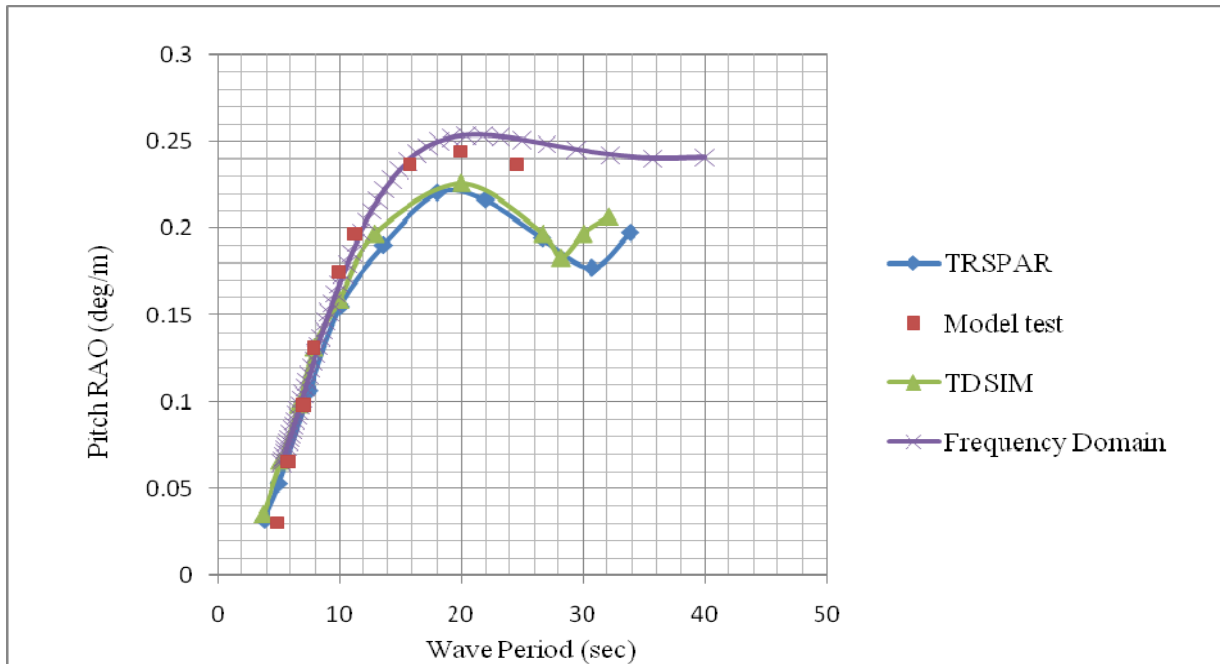


Fig. 8: Comparison of pitch RAO at zero degree heading

4. CONCLUSIONS

- 1) A MATLAB numerical program namely 'TRSPAR' was developed to determine the dynamic responses of a truss spar platform.
- 2) 'TRSPAR' has provision for calculating the hydrodynamic coefficients at any point of the structure and at any instant, based on the KC parameter. This provision was made use of for obtaining the numerical motion responses.
- 3) The above program 'TRSPAR' was applied to a proto type spar namely Marlin truss spar and the responses were compared with the frequency domain results, results of another numerical simulation called TDSIM and model test results on this spar. 'TRSPAR' results compared well with all the other three sets of results. Except for the differences in the heave response amplitude for higher wave periods, frequency domain results agreed well with the three sets of results.
- 4) Based on the above results, frequency domain analysis shall be considered as an approximate approach for calculating the dynamic responses of truss spar platform and it can be used for preliminary design.

REFERENCES

1. Prislun, I, Belvins, RD, and Halkyard, JE (1998). "Viscous Damping and Added Mass of Solid Square Plates." Proc 17th OMAE Conference, Lisbon, Portugal.
2. Troesch, AW, Perlin, M, and He, H (2000). "Hydrodynamics of Thin Plates," Joint Industry Report, U Michigan, Dept Naval Architecture and Marine Engineering, Ann Arbor.
3. Kim, MH, Ran, R, Zheng, W, Bhat, S, and Beynet, P (1999). "Hull/Mooring Coupled Dynamic Analysis of a Truss Spar in Time Domain," Proc 9th Intl Offshore and Polar Eng, ISOPE, Brest, France.
4. Luo, YH, Lu, R, Wang, J, and Berg S (2001). "Time-Domain Fatigue Analysis for Critical Connections of Truss Spar," Proc 11th Intl Offshore and Polar Eng, ISOPE, Stavanger, Vol 1, pp 362-368.
5. Wang, J, Luo, YH, and Lu, R (2002), "Truss Spar Structural Design for West Africa Environment," Proc. 21st OMAE Conference, Oslo, Norway.
6. Cao, P.M., (1996), "Slow Motion Responses of Compliant Offshore Structures," MS Thesis, Ocean Engineering Program, Civil Engineering Department, Texas A&M University, College Station, Texas.
7. Chakrabati, S.K., (2001), "Hydrodynamics of Offshore Structures," Computational Mechanics Publications, Southampton, Boston.
8. Paulling, J.R.(1995), "TDSIM6: Time Domain Platform Motion Simulation with Six Degrees of Freedom. Theory and User Guide," 4th Ed.
9. A.K. Agarwal, A.K. Jain.(2002), "Dynamic behavior of offshore spar platforms under regular sea waves," Journal of Ocean Engineering.